

A Review of Lung Cancer Analysis Using Artificial Intelligence And Deep Learning Algorithms

B.Durgalakshmi¹, M.Deepika²

Tagore Institute of Engineering and Technology, Salem, Tamil Nadu, India.

Abstract

Lung cancer is a fatal disease with a high mortality rate in diseased patients. Early diagnosis of this disease and accurately identifying the lung cancer stage can save the patients' lives. Several image processing, based and machine automation approaches are used to identify lung cancer, but accuracy and early diagnosis are challenging for medical practitioners. The Lung Image Database Consortium and Image Database Resource Initiative are utilized in this study to extract the CT scan images. In conventional methods, manual CT images are supplied to visualize whether the person has lung cancer. This research article proposes a novel method for early and accurate diagnosis called cancer cell detection using hybrid neural networks and other algorithms. The features are extracted from the CT scan images using deep neural networks. The accuracy of feature extraction is very important to detect cancerous cells at early stages to save the patient from this fatal disease.

Keywords: Lung disease, Machine learning, Hybrid neural network, Diagnosis of lung cancer.

Introduction

The development and spread of aberrant cells throughout the body is cancer. The specific etiology of the illness is yet unknown. Bad behaviors like smoking or drinking may bring that on or be inherited and immune system-related. Both the rate of global cancer incidence and the rate of technological advancement are accelerating nowadays. Our research is motivated by the effectiveness of using CNN algorithms in digital pathology image processing, as previously described, and intends to further discover the high level and discriminative properties shown by cancer cells using CNNs for exact categorization of lung cancer subtypes. Only after carefully reviewing CT images, which take a lot of time and are not always accurate, can doctors make the diagnosis of lung cancer. The body's cancerous cells grow faster than healthy cells, causing lumps to develop into nodules or tumors. In this paper, the first objective is to analyze and detect the cancer cells using an advanced 3D-Convolutional Network (3D-CNN) with recurrent neural network (RNN). Lung nodules are round or oval lung tissue lumps with a diameter of less than 30 mm that may be seen on CT scan images. They stand for different shapes, densities, places, and surroundings. As seen in Fig. 2(a) and (b), the width of lung nodes often exceeds 3 mm; nodes with a diameter of less than 3 mm are referred to as micro nodes. As non-nodules that mimic nodules, pulmonary and vascular walls might cause false detections (Fig. 2(c)). According to their concentration, lung nodules may be categorized into three groups: solid lesions, ground glass ware, and partially solid nodules (Fig.2(d,e,f))[5,6]. According to Fig. 2(d), (g), or (h), nodes might have solitary, juxta-pleural, or juxta-vascular terminal positions. Nodules are usually difficult to discern when there is pulmonary edema (Fig. As a consequence, precisely identifying and diagnosing lung nodules has become much more difficult. Small-cell lung cancer (SCLC) and non-small-cell lung cancer (NSCLC) are both types of lung cancer. 75% of lung cancer cases are NSCLC; however, not all clusters are tumor cells; those less than 3 mm in diameter are benign tumors, while those more than 3 mm in diameter progress to malignancy [5, 6]. Computer-aided diagnostic (CAD) technologies

are used in medical science to detect diseases in the early stages [7]. Radiologists and physicians used to diagnose a variety of diseases using the CAD methods [8]. Early phases of certain diseases, such as lung, skin, and prostate cancer, are typically not detected easily. Therefore, the CAD system is useful for detecting cancer in its early stages. The performance of the system is measured in terms of precision, velocity, and automated level [9]. Compared to x-ray pictures, CT scan images are more useful in diagnosing malignant lung nodules [9]. X-rays are used to locate specific bodily parts, not tumors. When the CT scan pictures are rotated to cover a 360-degree region, nodules with bones attached are discovered. Finding small lung anomalies aids in inaccurately diagnosing patients by radiologists [10]. Only manual CT identification is practical if you require correct information from the scanned picture. However, a machine learning (ML) algorithm is required to identify the cause of the disease at an early stage. There are two approaches to finding pulmonary nodules. The lung endothelium is first removed from the CT-scanned picture to identify tiny nodules in the chest from the pulmonary vasculature [11]. To reduce the mortality rate of cancer, it is imperative to focus greater emphasis on the health sector and, in particular, to develop innovative mechanisms for early cancer detection. When employing cancer segmentation data, segmentation accuracy is a crucial factor to take into account. Due to inter-observer variability and inconsistent methods, radiologists can create inaccurate findings when segmenting images manually. An automated segmentation technique of lung cancer Images from CT scans is very pertinent to solving this issue.

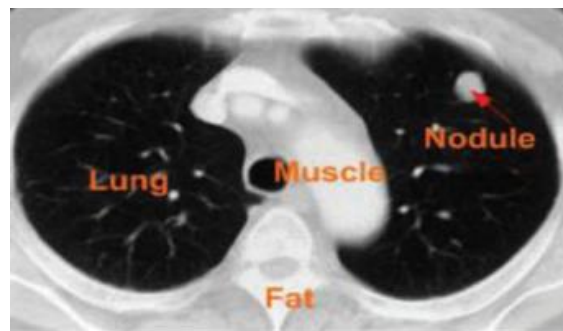


Fig. 1. CT scans image of the patient with lung cancer.

1.1. Related works

The different cancer detection models using machines and DL models are analyzed and listed in this section. Based on the analysis, the fundamental issues in cancer detection and classification are identified to design a new framework. The paper suggested a DL approach in this study to identify and categorize breast tumors in chest cytology scans using the idea of domain adaptation [12]. DL algorithms are typically executed in sequence and are modeled to be task-specific. Transfer learning aims to apply the knowledge acquired while solving the issue, in contrast to classical training models developed and produced in isolation. The proposed system employs pre-trained CNN models to retrieve images that contain features. These structures are then supplied into a fully coupled layer for categorizing malicious and benign molecules using ordinary pooling. The suggested system uses Balance Contrast Enhancement Technologies (BCET) to increase features and gain features of medical pictures for a correct diagnosis, giving a unique method for detecting breast tumors [13]. The outcomes of the second phase are then subjected to image classification using the fuzzy c-means (FCM) clustering approach and holding technique to determine the limits of the breast tumors (form, size, geographical sizes, etc.) and segment the outside limits of the breast. The third phase of extracting features involves utilizing discrete wavelet transformation (DWT). Ultimately, the classification of the phase of a breast tumor as benign, aggressive, or healthy will be done using a synthetic neural network. The likelihood of surviving will increase with early breast cancer discovery. This paper offered an improved automated decision-assisting system for lesion identification and categorization based on multivariate region-based fully convolutional networks (mRFCN) [14]. In [15], the innovative multi-Layer Region Prediction Network (mLRPN) and the mRFCN are used as the foundation of the image classifiers for extracting features, and position-sensitive rating maps are being investigated. It used a median brightness projection to use the three-dimensional data from computer tomography (CT) scanners. added-

convolutional level to automatically incorporate the suggested mLRPN in the design to choose the possible regions of interest. This research provides a framework for identifying and classifying cancerous tissue in breast tumors using breast cytology images and a cloud-based decision support system [15]. In [16], the proposed approach uses shape-based characteristics to recognize tumor cells. Additionally, these traits are used to classify cells into categories of healthy and cancerous cells by Naive Bayesian and Artificial Neural Networks. Another important step that the suggested framework addresses is rating the damaged cells. That might make it easier to evaluate crucial patient care procedures during clinical evaluation. To demonstrate the efficacy of the suggested method, experiments are conducted on data sets comprising patient information that was obtained from the pathologist. In [17], the article provided a comprehensive review of lung cancer using DL techniques. The authors conducted a literature evaluation of papers from various conferences and journals by searching databases from Science Direct, IEEE Xplore, Springer Link, Google Scholar, and Wiley. The system design architectures of various techniques and methods for detecting lung cancer cells have been examined, and their efficacy has been assessed. In [18], the article implemented a DL approach based on the U-Net and ResNet34 architectures. In order to evaluate the system, four different kinds of datasets were used. The dice similarity coefficient (DSC), a performance measure, was calculated and found to be greater than 0.93. They verified that there was a slight decline in consolidation while analyzing two pathological instances. This paper provided an example of a technique that generates F-scores between 99.2% and 99.3%. The recommended approach evaluates the illness using success metrics. This paper provides an example of a technique that generates F-scores between 99.2% and 99.3%. In [19], using image fusion to segment the nodule, the authors demonstrated an improved method for detecting lung cancer cells. An integrated fusion method, based on a Laplacian pyramid (LP) decomposition with an adaptive sparse representation, is presented in the article [20]. The method was successful because it could be divided into various shapes. Here, the segmented sizes were combined into four layers using the LP technique. The dataset was used to assess the model, and the DSC performance measure was calculated; it was almost 0.99%. In [21], the authors developed a machine that can quickly detect lung cancer using a manual approach. They used a dataset of 1800 images, including 900 images of children diagnosed with lung cancer, as well as CT images and a Gabor filter. However, the authors did not provide any information on the success rate of their method. On the other hand, the authors also developed a CAD model that was tested on three datasets and achieved an average accuracy of 99.42% and the highest accuracy of 99.61%. The CAD model also showed high F-score, recall, and precision, with results of 99.76%, 99%, and 99%, respectively. In [22], the objective of this research is to determine whether a patient's lungs have been affected by cancer. Techniques for statistical learning and image processing were used by these systems to function. The algorithms were tested on a batch of 198 photos from the Kaggle website. It achieved an accuracy of around 72.2%, which is much lower than the technique analyzed in this article's accuracy of 99.42%. The suggested method in this study successfully achieves recall, precision, and the F-score with scores of 99.76, 99.88, and 99.82%, respectively. These excellent findings show that this method is preferable to the one that was employed. The implemented approach in [6] employed one dataset with 198 photos; however, the system reported in this study only used three datasets with 1463 images for testing. In [23], the authors present Sybil, a DL model that predicts a person's future risk of developing lung cancer using a single low-dose computed tomography (LDCT) scan without any need for further clinical or demographic information. In external validation sets, the model has demonstrated good accuracy and has the potential to provide individualized screening. But further investigation is required to comprehend its clinical uses. Separation, feature extraction, categorization, and image preprocessing are the four major components of the proposed method [24]. Laplacian filtration, which was originally employed to identify the edges in mammography images, was particularly noise-sensitive. The image was segmented using an ML algorithm, and a new technique was employed [25]. Using conventional methods, it was difficult to distinguish the poorly defined tumors in a mammogram image. To get around this problem and improve classification effectiveness, the correlation function was used in lieu of the distance measure. In order to extract specific features, the hybrid classification method was used to segment cancer areas [25]. In [26], the authors suggested a DL model to test the precision of lung cancer prediction using CT scan images. The study's main selling point is the decrease in false positives (FPs), and they used U-Net and 3DCNN to screen for FP nodules with high accuracy. In, the authors used CNN with RNN. They used CT scans taken before and after radiation therapy to train their CNN model to forecast survival. In their research, they were able to

monitor tumors and predict survival and prognosis at one and two years of overall survival using CNN and RNN models. Using SVM classifier, the authors suggest a viable and effective prototype model for the early identification and treatment of lung cancer. With a 98.8% accuracy rate, the model surpassed current SVM and SMOTE approaches in tests utilizing several cancer datasets. The suggested concept has the potential to enhance healthcare delivery and provide patients with lung cancer anywhere in the world with real-time, affordable therapy. Using genetic, clinical, and demographic data, the authors of [29] describe research on developing prediction models for the recurrence and survival of lung and squamous cell carcinoma patients. Three ML algorithms—decision tree approaches, neural networks, and support vector machines—are compared for accuracy and advantages in the research. The findings demonstrate that although decision tree models do not significantly improve accuracy, they do highlight the most important predictors in the input data, enabling doctors to make more personalized choices for patients. Continuous monitoring for lung cancer prediction modeling has been suggested by the authors [30]. To do this, the authors used a classification technique with fuzzy cluster-linked augmentation. For accurate image segmentation, the fuzzy clustering method is necessary. The use of ML methods, especially Naive Bayes (NB) and SVM classification algorithms, is recommended by the authors in [31] for identifying lung cancer in its early stages. The research emphasizes the value of early diagnosis and the possibility of using ML to comprehend illness trends. Both systems' accuracy is compared, offering helpful information for future field study. In [32], lung cancer cells are being studied using DL approaches. Lung cancer, the most common kind, accounts for a disproportionately high number of fatalities. A computed tomography (CT) scan image was used to estimate the chance that a person will get lung cancer. Nodules are the development of early tissue and are thought to be a common indication of cancer. In [33], authors built an ML model for estimating the risk of lung cancer in a large sample of patients who are younger. The model performed well and identified a high-risk group that made up 10% of lung cancer patients. The model is open for widespread dissemination and use; however, when using ML techniques, racial discrepancies must be considered. In [34], the author provides a summary of lung cancer and publicly accessible benchmark datasets for scientific investigation. It examines the current studies utilizing DL algorithms to analyze medical images for lung cancer and covers several methods for detection and classification. The study's conclusion highlights the clinical, technological, and future developments in this area. The diagnostic test precision of AI-based imaging for lung cancer screening is evaluated by the author in [35]. The evaluation comprised 26 studies with 150,721 imaging data points, and the findings point to the possibility of using AI-based imaging to identify lung cancer with a pooled sensitivity and specificity of 94.6% and 93.6%, respectively. However, the general quality of the evidence was quite poor, necessitating further credible research. In order to accurately and effectively diagnose lung cancer, the authors [36] presented the Lung Net-SVM model for automated module identification techniques in CT scans. On the LuNA16 dataset, the model demonstrated outstanding performance with 97.64% accuracy, 96.37% sensitivity, and 99.08% specificity. In [37], the author used a significant amount of real-world data and ML to create a 3-year lung cancer risk prediction model. The model proved transportability to EHR and claimed data and identified a high-risk group with a lung cancer incidence nine times higher than the average cohort incidence. By automatically identifying high-risk patients, the model's availability on an open-source platform might reduce the workload placed on physicians. In [38], the author validates the use of CXR-LC, an open-source DL tool, to identify high-risk individuals for lung cancer screening using EMR data. People with a high risk of lung cancer were detected by CXR-LC, including those who were ineligible per the most recent CMS recommendations. The use of CXR-LC could increase screening participation and perhaps lower lung cancer mortality. Based on the analysis, a new cancer identification and classification model is needed to increase the efficiency and accuracy of detecting cancer. A hybrid neural network based on cancer cell detection and classification is designed in this research to detect cancer and classify the severity of the disease. The motivation is to address the challenges of accurately identifying and diagnosing lung cancer at an early stage, as well as improving the accuracy of distinguishing between benign and malignant tumors.

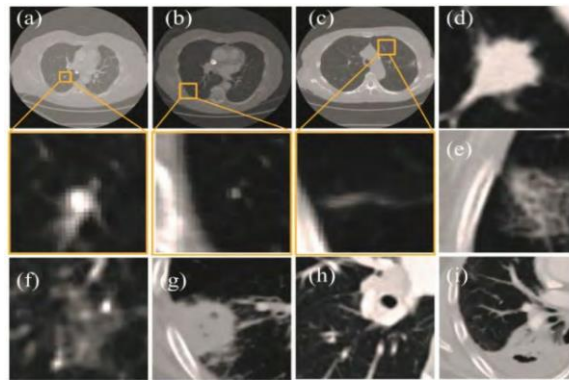


Fig. 2. Illustration of a wide variety of lung nodules

1.2. Objectives

The objective of the research is to introduce a new technique called CCDC-HNN that utilizes a combination of deep neural networks to detect lung cancer at an early stage and with high accuracy using CT scan images. The approach involves extracting features from the images through deep neural networks and employing advanced 3D-CNN to enhance the precision of the diagnosis. Additionally, the proposed technique aims to distinguish between benign and malignant tumors. The study intends to assess the outcomes using established statistical methods and establish the feasibility of the proposed hybrid DL approach for the timely detection of lung cancer. The rest of the paper is structured in the following way: In Section 2, we provide an overview of the background to cancer cell detection and classification models. We present our proposed approach, which is called Cancer Cell Detection and Classification using Hybrid Neural Networks (CCDC-HNN) in Section 3. In Section 4, we discuss our analysis of the software and evaluate the performance of our framework. Using specific metrics. Finally, we conclude the paper in Section 5 and suggest directions for future research.

2. Proposed methodology

CNN-RNN can be employed to evaluate digital histopathology images since they contain many pixel data. This study presented a combination CNN-RNN system that concentrated on visuals to give a broad context. The suggested approach first converts a histological picture's regional representation into a higher-dimensional characteristic and then aggregates the feature by assessing its spatial organization to allow the final forecasts. The images from formalin-fixed, paraffin-embedded diagnosed blocks of malignant skin conditions were taken from Genome Sequencing and used as the database. This suggested model analyzes histological pictures to evaluate melanoma tumors using CNN-RNN.

Major research contributions:

- Proposes a novel method called Cancer Cell Detection using Hybrid Neural Network (CCDC-HNN) for early and accurated diagnosis of lung cancer. Lung Image Database Consortium and Image Database Resource Initiative (LIDC-IDRI) to extract CT scan images for the Uses deep neural networks to extract features from the CT scan images, which are crucial for the accurated detection of cancerous cells at early stages.
- utilizes an advanced 3D-convolutional neural network (3D-CNN) to further improve the accuracy of diagnosis.
- Enables the distinction between benign and malignant
- Demonstrates the viability of the proposed hybrid DL technique through evaluation using standard statistical techniques.

2.1. Hybrid classifier

The classification of the pictures into healthy, abnormal, and cancerous uses a hybrid of CNN and RNN. The suggested model is developed into a mixed CNN and RNN method using an optimized hidden layer approach. CNN: Multiple layers, including the convolution layer, max pooling, and one or even more completely connected layers, make up the basic framework of CNN. Three layers are combined in this process. Information is shared from the source to the production side in CNNs. Convolutional layers: They function as extractors; these layers aid in learning the representations of image pixels. Information maps are created by the neurons. The convolutional filter associated with the functionality map is signed by The 2D convolution layers driver Is signified by*, which is used to measure the inner outcome of the filtration in every feature of the input picture, to calculate the efficiency functionality map for Co . The nonlinear features for the filter is denoted d in Eq. (1).

$$Co = f(m \times X) \quad (1)$$

The activation function is denoted f , and the input image is denoted X . The two functions, like sigmoid and nonlinear activation, are frequently used. The spatial granularity is reduced using the image reflection to achieve spatial normalization to input rotations and deformation. It is customary to use common pooling levels to transfer the typical input data of the small area of a picture. Every resultant map combines the Convolution from all of the input mappings. The convolutional layer output is denoted in Eq.(2). The previous convolutional layer output is denoted Co_{l-1} . The kernel function and additive bias function are denoted as K^{CL} and AB^{CL} . The maximum number of input images and processing layers are denoted by N and M . Fully interconnected layers: A modular multilayer network is part of CNN's ultimate stage. Many layers are stacked together to obtain the abstract component representations by traveling in the system. For high-level cognitive tasks, this kind of layer mimics the features of pooled and convolutional levels.

Training To change the public variables and achieve the desired net-work result, RNNs and CNNs require DL. The back propagation is typically used for this aim.

RNN: It is a subtype of CNN in which a structure called the development of data is formed by the connections between the nodes. As a result, the outcome seems to be the best when identifying the current and older data since it can deal with time information efficiently. One RNN type that uses memory cell units is Long Short Term Memory (LSTM). Input, memory, and output gateways make up its three gate units. Furthermore, the gradients, masses, and explosions are resolved using LSTM. The LSTM efficiently eliminates the extraneous data and grabs the critical information in series after refreshing the state of the storage cell unit by triple gates.

GRU is a unique variety of LSTMs utilized to construct the RNN model to improve performance. GRU combines the outcome and forget gates into a single update gate, where interpolation aids in obtaining the current result. The updated gate function and recurring gate function are denoted in Eq. (3) and (4). The predicted hidden layer outcome and the previously hidden layer results are denoted as H_k and H_{k-1} . The linear weight of the activation is denoted by d as Ug . The suggested technique optimizes amount of concealed layers in CNN and RNN. The final categorized output is produced by applying the AND function to the CNN and RNN results. Thus, the three classes normal, benign, and malignant are derived from the mammography pictures used as input.

2.2. Data preparation

The system uses the publicly accessible LIDC/IDRI dataset's component, the LUNA16 dataset. Use the patient's CT scan kit to examine the nodules and create a u-net for lung nodule identification using the lung nodule analysis 2016 challenges. The size 710 training sample and size 178 validation set are divided across the 888 individuals labeled information in the LUNA 16 kit. Each participant has nodule tags and computed tomography (CT) data (list of coordinates and nodule center diameter). Each participant's CT scan data comprises 512×512 pixel pictures of various sizes (ranging from 100 to 400). A U-Net on nodule identification was formed at each stage of our classification procedure using the LUNA16 information. Fig. 3 indicates the architecture of the system. The proposed CAD system begins with preprocessing 3D CT scan images using segmentation, normalization, noise removal, grayscale image, and enhancement. The first approach was inserting the preprocessed 3D CT image into the 3D CNN, but the results were terrible. Therefore, additional preprocessing was performed to identify the region of interest in the 3DCNN. U-Net nodes were trained to identify nodule candidates, detected, and regions of interest. The five levels of dangerous and innocent lung cancer, 2, 3, 4, and 5 are defined by the LIDC-IDRI database standards. The number "3" indicates that the relevant node's status is unknown. Node "3" was therefore handled in two separate ways: (i) it was divided into nodes "1" and "2", which were designated as innocuous. (ii) As in the aggressive category, divided by the numbers "4" and "5". The ROI of the nodule chosen for this investigation is these overlapped regions, which combine four locations recognized by a radiologist, as depicted in Fig. 4. This removes discrepancies in the information. Since the observed nodules with a diameter less than 3 mm are less critical, this study mainly chooses nodes with a range of 3–30mm. Lung nodes are first grouped into labels issued by experts, and then images are normalized. For choosing the 56×56 normalization constant is that this study showed that the maximum node diameter r does not exceed 55 pixels. Fig.5 shows some typical lung nodule morphology. It describes five different lung nodule types.

2.3. Feature extraction

The most significant data from the image gives a more thorough picture of knowledge. The definition of a function is one or more measuring functions that target some calculated qualitative real estate values that object to the characteristics based on geometry and intensity are retrieved. This measurement data may help in determining if a lung nodule is cancerous or not. A physical aspect used to describe an object's geometry is shape measurement. Perform training and testing on the extracted pictures after retrieving the feature. When fitting a model during training, the method incorporates a classification classifier, and the variable is the performance prototype, which is only evaluated when test data is utilized. The test data must be anticipated since it is unknown, yet the outcome of the training examples may be simulated. The retrieved photos are evaluated, learned from, and classified using data.

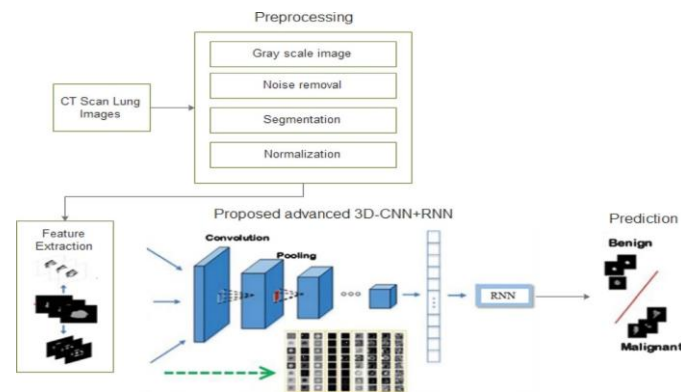
2.4. Proposed advanced 3D-CNN with RNN for classification of lung CT

Identifying whether a nodule is regular or malignant is important once the prospects for nodules have been removed from the picture. After training and evaluating the information, the system conducts the categorization by applying a 3D-CNN+RNN classification. Kernel size in all convolution and combined layers should be considered, such as $3 \times 3 \times 3$ and $2 \times 2 \times 2$, respectively. Also, the number of cores plotted in the convolution layers on the function maps is 96, 128, 256, 324, and 512, respectively. First convolution layer, 96 filters by $3 \times 3 \times 3$ filters apply input images $227 \times 227 \times 227 \times 227$ sizes, and the max-pooling redundancy level minimizes the production size of the existing convolution layer by using filtration. Object maps with reduced sampling pass through the second and third convolution layers. The second layer of the union was applied to control the down sampling on the output map of the objects of the third convolution layer. The last convolution layers were used for the down-sampled function map. The build is about layers that are fully connected to the layers that connect the nerve cells of the previous layer. RNNs are types of neural networks that are output from the previous transfer step as input to the current step. Here the same parameters are used for each input because the expectations were to perform the same task on all inputs or hidden layers to get the output. Images from CT scans of lung nodules are examined. The initial detection,

therapy, and maintenance of lung cancer were improved when 3D-CNN+RNN were used to identify pulmonary nodules and classify them as dangerous or normal.

2.5. Training model

Pre-trained convolutional neural system layers, RNN layers, Merging merging layers, and utterly connected surfaces with Softmax output make up the proposed model. For training, the model's back propagation is mainly preferred.



2.5.1. Pre-trained convolutional neural network layer

The system uses the feature weights obtained from pre-training on the Image Net database as the starting weights for CNN architecture. Convolutional operation and max pooling are components of convolutional networks.

2.5.2. Convolutional layer

The primary method for calculating this layer is the most crucial component of the convolutional network. It is to employ convolution windows of various sizes to execute convolutional filters with the extracted features from the previous layer. Sequentially convolutional windows are slid onto the last layer. Typically, the convolutional layer has three or five feature weights depending on the time window, which is 3×3 or 5×5 . The activation function utilized in the layer is used to achieve the result in the convolution operation twisted through matching windows.

2.5.2. Pool layer

This layer operates similarly to the convolutional layer in terms of calculation. The distinction is that the lowest layer's sliding window is typically 2×2 , and the slipping step is 2. Because of this, the width of the last layer's feature space is typically cut in half. That effectively reduces the convolutional weights within the neural system parameters, which helps accelerate the network training phase. Additionally, it enables the system to be more adaptable to the size of the picture modifications at the exact moment. This study applies the pre-trained network and the Linear Rectification Function. Another enhanced version of Google's Inception v3 is called Xception. It primarily provides depth-wise separation to sweep out the convolution techniques seen in the initial model. As an upgraded version of Inceptionv3, Xception includes depth wise separable compression, which enhances the model's performance without adding to the system's intricacy.

2.5.4. RNN layer

An input level, a hidden surface, and an output surface are present in both RNN and CNN. The most crucial aspect of RNN is how these hidden layers are connected. The concealed layer is sent to the output

nodes by connecting the input level nodes and the concealed layer vertices. Even for the concealed state, neighbors to one another are included in the node outputs data sent back to the concealed layer node. RNNs are depicted as being closer to the natural neural networks, which are cyclic systems that can comprehend serial communication [39]. This method can learn from long-term reliance. LSTM differs from RNN by including a “processor” to judge whether the data is helpful or not. Input gates, the memory gate, and the gate of output are the three doors positioned in a cell. A message joins the LSTM model and is subject to rule evaluation. The inconsistent data is erased via the Oblivion Gate, leaving only the data that has been certified by the program. A memory cell plus three multiplicative gates, namely input, outputs, and for get gates. The LSTM features a more intricate structure than the typical RNN module.

2.5.5. Merge layer

The merger layer function combines the characteristics received from the RNN and those acquired from the CNN using a particular technique. The merge layers function combines the data received from the RNN and the characteristics acquired from the CNN using a particular technique. A neural network that can pick a particular input and concentrate on it (or its characteristics) is said to have a neural network learning algorithm. For feature merging, the system applies the appropriate element-wise multiplying procedures [40].

2.5.6. Fully connected layer with a Soft max output

The probability distributions of fall categories result from the densely integrated Soft max level, which receives the features produced by the RNN and CNN after they have been combined. The cross-entropy is also used as an error function to calculate the discrepancy between the actual and desired output.

2.5.7. Network training

The RNN branch initializes the variables arbitrarily, while the values in the CNN node use values that have been pre-trained on the Image Net database. Through the slope of the cross-entropy error function, these values are continuously adjusted during the training phase. First, the CNN layer is locked. The optimizer then calculates the training data, which takes ten iterations. The CNN level is defrosted, the Adam optimizer is used throughout the system to compute training data, the development rate is set to 0.001, and 10 epochs are needed for training. After a specified number of intervals, the training procedure ends. The version with the smallest value of validation loss was selected as the final network. The proposed CCDC-HNN framework is designed in this section, and the outcomes are verified with the mathematical model. The CCDC- HNN frame work with a hybrid 3DCNN and RNN model enhances cancer cell detection and classification outcomes. The simulation outcomes of the proposed system are verified in the next section.

2.6. Advantages of the proposed methodology

- Early and accurate diagnosis of lung cancer using CT scan images can improve patient outcomes and increase the likelihood of successful treatment.
- The use of deep neural networks for feature extraction, which can improve the accuracy of cancer cell detection compared to manual methods,.
- The incorporation of an advanced 3D-CNN can further enhance the accuracy of diagnosis and enable the distinction between benign and malignant tumors.
- The proposed hybrid DL technique shows promising results for the early diagnosis of lung cancer, as demonstrated by the statistical evaluation of the results.
- The proposed approach has the potential to be used in clinical practice, which could improve the efficiency and effectiveness of lung cancer diagnosis and treatment.

2.7. Architecture diagram of the proposed work

The work flow of the proposed CCDC-HNN frame work is shown in Fig.6. The necessary images for the analysis are accessed from the dataset, and the images are preprocessed. The dataset is segmented into training and testing samples using the hybrid neural network, and the proposed CCDC-HNN is trained and tested. Dataset examples were originally preprocessed in the segmentation method to identify the photos’ basic features. The training and evaluation sets were then created from the dataset. The validation data were classified using an RNN decoder and a pre-trained CNN structure.

2.7.1. Algorithm flow

The hybrid neural network-based cancer detection framework is shown in Fig.7. The necessary inputs for the analysis are taken from the dataset and preprocessed. The training samples are trained using CNN and RNN, and the testing results are analyzed using both methods. The predicted output from CNN and RNN is combined, and the final result is predicted. The exact process is repeated until the maximum threshold is attained. The optimized results are enhanced using the feedback in hidden layer weights.

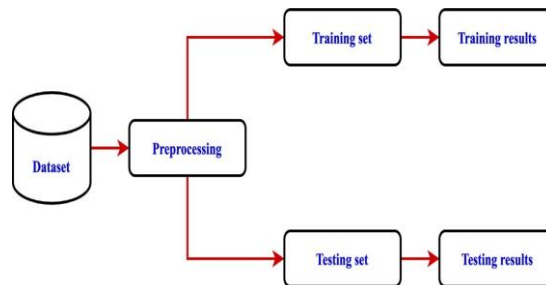


Fig. 6. Workflow of the proposed CCDC-HNN

2.7.3. Time complexity

The time complexity of a deep neural network (DNN) and 3D CNN depends on various factors, such as the number of layers, the number of neurons in each layer, the input size, and the type of activation functions used. The time complexity of a neural network is typically calculated by multiplying the number of operations required to compute a single forward pass by the number of forward passes required during training. Researchers today encounter a significant problem with the time complexity of any CNN model. Experts can assess the effects of each hyper parameter selected for a model’s construction by determining its time complexity. In our research, reducing the complexity of the dataset is essential to improving the diagnosis of lung cancer. Therefore, we use the feature selection method to separate the ideal lung features from a group of characteristics. The formula in Eq. (7) can be used to determine the time complexity of the completely connected layer.

$$TC = (\sum \sum ll = 1 ff DD. WW. HH. NN) \tag{7}$$

Here,"l" represents the depth of the fully connected layer, while “D”, “W”, “H”, and “N” define the dimensions of the input/output channel, the width of the input, the height of the input, and the number of outputs, respectively. It is not necessary that a model with a higher number of layers will also have a higher computational complexity. In real-time implementation, the computation time complexity depends on the layered approach used. In the proposed algorithm, the DNN and 3D-CNN are utilized to extract features from CT scan images and improve the accuracy of diagnosis, respectively. The number of layers and neurons in each layer for both networks is not mentioned in the given information. However, it can be assumed that the proposed algorithm would require a significant amount of

computational resources due to the high complexity of these models and the large size of medical images. It is important to note that the time complexity of a deep neural network can be reduced by using techniques such as parallelization, transfer learning, and pruning, which are on our future research agenda. The discussed research paper proposes a novel method for early and accurate diagnosis of lung cancer using a hybrid DL approach called CCDC-HNN. The next section discusses the results. Fig. 7. Hybrid neural network-based cancer detection framework.

CONCLUSION

In this article, our goal is to propose a deep learning-based approach to classify pneumonia from chest X-ray images using transfer learning. In this framework, we adopted the transfer learning approach and used the pretrained architectures, VGG16 and ResNet trained on the ImageNet dataset, to extract features. These features were passed to the classifiers of respective models, and the output was collected from individual architectures. Finally, we employed an ensemble model that used pretrained models and outperformed all other models. We observed that performance could be improved further, by increasing dataset size, using a data augmentation approach, and by using hand-crafted features, in future. Our findings support the notion that deep learning methods can be used to simplify the diagnostic process and improve disease management. While pneumonia diagnoses are commonly confirmed by a single doctor, allowing for the possibility of error, deep learning methods can be regarded as a two-way confirmation system.

In this case, the decision support system provides a diagnosis based on chest X-ray images, which can then be confirmed by the attending physician, drastically minimizing both human and computer error. Our results suggest that deep learning methods can be used to improve diagnosis relative to traditional methods, which may improve the quality of treatment. When compared with the previous state-of-the-art methods, our approach can effectively detect the inflammatory region in chest X-ray images.

REFERENCES

1. Liu, N.; Wan, L.; Zhang, Y.; Zhou, T.; Huo, H.; Fang, T. Exploiting Convolutional Neural Networks With Deeply Local Description for Remote Sensing Image Classification. *IEEE Access* 2018, 6, 11215–11228.
2. Litjens, G.; Kooi, T.; Bejnordi, B.E.; Setio, A.A.A.; Ciampi, F.; Ghafoorian, M.; van derLaak, J.A.W.M.; Ginneken, B.; Sánchez, C.I. A survey on deep learning in medical image analysis. *Med. Image Anal.* 2017, 42, 60–88. [PubMed]
3. Brunetti, A.; Carnimeo, L.; Trotta, G.F.; Bevilacqua, V. Computer-assisted frameworks for classification of liver, breast and blood neoplasias via neural networks: A survey based on medical images. *Neurocomputing* 2019, 335, 274–298.
4. Asiri, N.; Hussain, M.; Al Adel, F.; Alzaidi, N. Deep learning based computer-aided diagnosis systems for diabetic retinopathy: A survey. *Artif. Intell. Med.* 2019, 99.
5. Zhou, T.; Thung, K.; Zhu, X.; Shen, D. Effective feature learning and fusion of multimodality data using stage-wise deep neural network for dementia diagnosis. *Hum. Brain Mapp.* 2018, 40, 1001–1016.
6. Shickel, B.; Tighe, P.J.; Bihorac, A.; Rashidi, P. Deep EHR: A survey of recent advances in deep learning techniques for electronic health record (EHR) analysis. *IEEE J. Biomed. Health Inform.* 2018, 22, 1589–1604.

7. Meyer, P.; Noblet, V.; Mazzara, C.; Lallement, A. Survey on deep learning for radiotherapy. *Comput. Biol. Med.* 2018, 98, 126–146. *Appl. Sci.* 2020, 10, 559 15 of 17
8. Malukas, U.; Maskeliūnas, R.; Damaševičius, R.; Woźniak, M. Real time path finding for assisted living using deep learning. *J. Univers. Comput. Sci.* 2018, 24, 475–487.
9. Zhang, X.; Yao, L.; Wang, X.; Monaghan, J.; McAlpine, D. A Survey on Deep Learning based Brain Computer Interface: Recent Advances and New Frontiers. *arXiv* 2019, arXiv:1905.04149.
10. Bakator, M.; Radosav, D. Deep Learning and Medical Diagnosis: A Review of Literature. *Multimodal Technol. Interact.* 2018, 2, 47.
11. Gilani, Z.; Kwong, Y.D.; Levine, O.S.; Deloria-Knoll, M.; Scott, J.A.G.; O'Brien, K.L.; Feikin, D.R. A literature review and survey of childhood pneumonia etiology studies: 2000–2010. *Clin. Infect. Dis.* 2012, 54 (Suppl. 2), S102–S108. [PubMed]
12. Bouch, C.; Williams, G. Recently published papers: Pneumonia, hypothermia and the elderly. *Crit. Care* 2006, 10, 167. [PubMed]
13. Scott, J.A.; Brooks, W.A.; Peiris, J.S.; Holtzman, D.; Mulholland, E.K. Pneumonia research to reduce childhood mortality in the developing world. *J. Clin. Investig.* 2008, 118, 1291–1300. [PubMed]
14. Wunderink, R.G.; Waterer, G. Advances in the causes and management of community acquired pneumonia in adults. *BMJ* 2017, 358, j2471. [PubMed]
15. National Center for Health Statistics (NCHS); Centers for Disease Control and Prevention (CDC) FastStats: Pneumonia. Last Updated February 2017. Available online: <http://www.cdc.gov/nchs/fastats/pneumonia.htm> (accessed on 21 November 2019).
16. Heron, M. Deaths: Leading causes for 2010. *Natl. Vital. Stat. Rep.* 2013, 62, 1–96.
17. World Health Organization. The Top 10 Causes of Death; World Health Organization: Geneva, Switzerland, 2017; Available online: <https://www.who.int/news-room/fact-sheets/detail/the-top-10-causes-of-death> (accessed on 10 November 2019).
18. Kallianos, K.; Mongan, J.; Antani, S.; Henry, T.; Taylor, A.; Abuya, J.; Kohli, M. How far have we come? Artificial intelligence for chest radiograph interpretation. *Clin. Radiol.* 2019, 74, 338–345.
19. Wang, X.; Peng, Y.; Lu, L.; Lu, Z.; Bagheri, M.; Summers, R.M. Chestx-ray8: Hospital scale chest x-ray database and benchmarks on weakly-supervised classification and localization of common thorax diseases. In *Proceedings of the IEEE Conference on Computer Vision and Pattern Recognition*, Honolulu, HI, USA, 21–26 July 2017; IEEE: Piscataway, NJ, USA; pp. 2097–2106.
20. Ronneberger, O.; Fischer, P.; Brox, T. U-net: Convolutional networks for biomedical image segmentation. In *Proceedings of the 18th International Conference on Medical Image Computing and Computer-Assisted Intervention*, Munich, Germany, 5–9 October 2015; Springer International Publishing: New York, NY, USA; pp. 234–241.
21. Roth, H.R.; Lu, L.; Seff, A.; Cherry, K.M.; Hoffman, J.; Wang, S.; Liu, J.; Turkbey, E.; Summers, R.M. A new 2.5 d representation for lymph node detection using random sets of deep convolutional Neural network observations. In *Proceedings of the 17th International Conference on Medical Image Computing*

and Computer-Assisted Intervention, Boston, MA, USA, 14–18 September 2014; Springer International Publishing: New York, NY, USA; pp. 520–527.

22. Shin, H.-C.; Roth, H.R.; Gao, M.; Lu, L.; Xu, Z.; Nogues, I.; Yao, J.; Mollura, D.; Summers, R.M. Deep convolutional neural networks for computer-aided detection: Cnn architectures, dataset characteristics and transfer learning. *IEEE Trans. Med. Imaging* 2016, 35, 1285–1298.

23. Rajpurkar, P.; Irvin, J.; Ball, R.L.; Zhu, K.; Yang, B.; Mehta, H.; Duan, T.; Ding, D.; Bagul, A.; Langlotz, C.P.; et al. Deep learning for chest radiograph diagnosis: A retrospective comparison of the CheXNeXt algorithm to practicing radiologists. *PLoS Med.* 2018, 15, e1002686.

24. Woźniak, M.; Połap, D.; Capizzi, G.; Sciuto, G.L.; Kośmider, L.; Frankiewicz, K. Small lung nodules detection based on local variance analysis and probabilistic neural network. *Comput. Methods Programs Biomed.* 2018, 161, 173–180.

25. Gu, Y.; Lu, X.; Yang, L.; Zhang, B.; Yu, D.; Zhao, Y.; Gao, L.; Wu, L.; Zhou, T. Automatic lung nodule detection using a 3D deep convolutional neural network combined with a multi-scale prediction strategy in chest CTs. *Comput. Biol. Med.* 2018, 103, 220–231.